EUROPEAN FUSION DEVELOPMENT AGREEMENT

EFDA–JET–CP(01)02-83

S.E. Sharapov, D.N. Borba, A. Fasoli, C. Giroud, A. Gondhalekar,
N.C. Hawkes, T.C. Hender, V.G. Kiptily, M.J. Mantsinen, F. Nabais, D. Testa
and JET EFDA Contributors

Beam Afterglow Scenario for TAE Excitation in Optimised Shear JET Plasmas

Beam Afterglow Scenario for TAE Excitation in Optimised Shear JET Plasmas

S.E. Sharapov, D.N. Borba[1,2], A. Fasoli[3], C. Giroud, A. Gondhalekar,
N.C. Hawkes, T.C. Hender, V.G. Kiptily, M.J. Mantsinen[4], F. Nabais[1], D. Testa[3]
and JET EFDA Contributors*

Euratom/UKAEA Fusion Association, Culham Science Centre, Abingdon, Oxon OX14 3EA, UK
[1]*Assoc. Euratom/IST, Av.Rovisto Pais, 1049-001, Lisboa, Portugal*
[2]*EFDA Close Support Unit, Culham Science Centre, Abingdon, Oxon OX14 3DB, UK*
[3]*Plasma Science and Fusion Centre, MIT, Cambridge, Massachussets MA02139, USA*
[4]*Helsinki University of Technology, Association Euratom-Tekes, Finland*
**See appendix of the paper by J.Pamela "Overview of recent JET results",*
Proceedings of the IAEA conference on Fusion Energy, Sorrento 2000

Preprint of Paper to be submitted for publication in Proceedings of the
EPS Conference,
(Madeira, Portugal 18-22 June 2001)

ABSTRACT

TAEs excited by α-particles in DT plasma can provide information about the pressure and slowing-down time of α's. A search for α-driven TAEs in JET [1] and TFTR [2] has shown that TAEs are difficult to excite during main NBI heating phase. The "beam afterglow" scenario for TAE excitation, in which purely α-driven TAEs were observed after switching off NBI, was developed on TFTR [3, 4] and is being investigated on JET.

COMPARISON OF THE SCENARIOS FOR TFTR AND FOR JET

The beam afterglow scenario is targeting in a reduction in β_α required for destabilising TAE under conditions of low ion Landau damping, reduced central magnetic shear, and high central safety factor. Best conditions for TAEs in TFTR [3,4]: $t_{SD}(NBI \cong 100ms < t < t_{SD}(\alpha) \cong 300 \div 400ms$ and NBI of very high power, $P_{NBI} \approx 30MW$, to obtain the high performance plasma [3]. JET uses combined NBI+ ICRH heating, often with LHCD pre-heat, in order to generate internal transport barriers (ITBs) [5, 6] in plasmas with elevated q(0). Two major effects, associated with LHCD and ICRH, are important for α-driven TAEs in JET: 1) LHCD generates an equilibrium with reversed magnetic shear [7]. At the early heating phase of the discharge, ICRH ions excite Alfvén cascades [8], while TAEs often are not seen at all; 2)Residual drive from ICRH-accelerated ions may be larger than or comparable to the α drive, even after both NBI and ICRH are switched off [1]. In order to assess the JET specific conditions for TAE stability in the afterglow phase, parasitic measurements and dedicated experiments on TAE excitation in the afterglow JET plasmas were performed. Instead of the fusion α's, ICRH-accelerated hydrogen minority ions were used in order to probe TAE stability in D plasmas. ICRH-driven TAEs in JET were studied earlier [9, 10], but no significant data on TAE excitation in the beam afterglow regimes existed so far.

TAE IN JET AFTERGLOW PLASMA WITH ELEVATED MONOTONIC q(r)

Two optimised shear (OS) scenarios are exploited on JET in order to generate ITBs:1) ITB is triggered by high power NBI+ICRF heating applied to a plasma with a monotonic q(r) [5]; 2) ITB is triggered at smaller power of NBI+ICRF heating, if a non-monotonic q(r) is generated by LHCD [6]. In the scenario with monotonic q(r), ICRH was applied in the beam afterglow phase with ICRH power gradually increasing up to 6MW (Fig. 1). NBI of small power was used for MSE and charge-exchange diagnostics during the afterglow phase. Figure 2 shows external magnetic measurements of TAEs with toroidal mode numbers $n=4$, $n=5$ and $n=6$ in the afterglow phase at $P^{crit}_{ICRH} \approx 3.8MW$.

ALFVÉN CASCADES AND TAE IN JET DISCHARGES WITH NON-MONOTONIC q(r)

Alfvén instabilities are very different at the early phase of two types of OS discharges. In case with monotonic q(r) -profile, ICRH drives TAE modes, while in plasma with nonmonotonic q(r) ICRH drives frequency sweeping Alfvén cascades below TAE frequency [8]. Comparison of Alfvén instabilities *at the late afterglow phase* of the discharges, when q(r) -profiles are relaxed, is an important issue for the beam afterglow scenario in JET. In order to assess the importance of Alfvén cascades and TAE in the afterglow phase of discharges with LHCD, experiments with LHCD were performed (Figs. 3,4).In order to avoid disruptions in discharges with non-monotonic q(r) - profiles, NBI was reduced from 13MW to 6.5MW only.

Figure 4 shows that although the early heating phase exhibit Alfvén cascades, TAEs with toroidal mode numbers from n=4 to n=9 are observed in the beam afterglow. We conclude that evolution of q(r) between the early heating and the afterglow phases was significant enough in order to make TAEs more unstable than the Alfvén cascades. Lowest TAE thresholds, $P_{ICRH} < 1.8$MW, were found in afterglow plasmas with nonmonotonic q(r).

CASTOR-K ANALYSIS OF TAE STABILITY

For all afterglow experiments MSE measurements of q(r) - profiles were performed (Fig. 5), together with measurements of ion and electron temperatures and density profiles. Energetic ion tails were measured by NPA and by γ-ray spectrometry. Radial profiles of energetic ions were computed by the PION code. On basis of the measurements above, CASTOR-K analysis of TAE stability is being performed. For typical afterglow case (Pulse No: 51773) plasma damping is not dominated by either bulk ion Landau damping, $\gamma_i/\omega \approx -0.12\%$, or the beam ion Landau damping, $\gamma_b/\omega \approx -0.28\%$, but is determined mainly by radiative and electron damping effects, $\approx (\gamma_R + \gamma_e)/\omega \approx -0.42\%$. The normalised growth rate γ_{ICRH}/ω for TAE driven by ICRH-ions is shown in Figure 6:

SUMMARY: TAE DATA BASE FOR AFTERGLOW SCENARIO.

In all the afterglow experiments TAEs of toroidal mode numbers varying in the range from $n = 3$ to $n = 9$ were successfully excited by ICRH. A data base was created for TAE:

1) Pulses *without LHCD*. ICRH power was added to beam ‘afterglow’’phase at different times, 0.1 and 0.4s, after beam TAEs were excited at’$\mathbf{(P_{ICRH})_{crit} = 3.8 \div 4.7}$**MW**.
2) Pulses *with LHCD pre-heating in order to invert/ to flatten q-profile*. ICRH power was added to beam ‘afterglow’’phase at 0.1, 0.4 and 0.8s after beam step-down. TAEs were excited at $\mathbf{(P_{ICRH})_{crit} = 1.8 \div 3.75}$**MW**.
3) Two pulses with NBI step-down power 13.3 → 8.4 → 6.7 → 2.9MW, at fixed ICRH power 2.9MW and **no Vbeam = VA/3 resonance**, and at fixed ICRH power 4.6MW and $\mathbf{V_{beam} = V_A/3}$ **resonance present**.

The spread of TAE excitation thresholds from 1.8MW to 4.7MW shows sensitivity of TAE stability mainly to q(r). CASTOR-K modelling is in progress for comparing theory and experiments. This work is a promising prelude to studies of α-driven TAEs in JET.

ACKNOWLEDGEMENT

This work has been conducted under the European Fusion Development Agreement and is partly funded by Euratom and the UK Department of Trade and Industry

REFERENCES

[1]. S.E. Sharapov et al., Nuclear Fusion 39 (1999) 373;

[2]. S.J. Zweben et al., Nuclear Fusion 36 (1996) 987;

[3]. R.V. Budny et al., Nuclear Fusion 32 (1992) 1497;

[4]. R. Nazikian et al., Phys. Rev. Lett. 78 (1997) 2976;

[5]. C. Gormezano et al., Phys. Rev. Lett. 80 (1998) 5544;

[6]. C. Challis et al., Plasma Phys. Contr. Fusion, to be published (2001);

[7]. N. Hawkes et al., submitted to Phys. Rev. Lett. (2001);

[8]. S.E. Sharapov et al., EPS Conference, Madeira (2001);

[9]. A. Fasoli et al., Plasma Phys. Contr. Fusion 39 (1997) B287; [10] A.Fasoli et al., Phys. Rev. Lett. 81 (1998) 5564

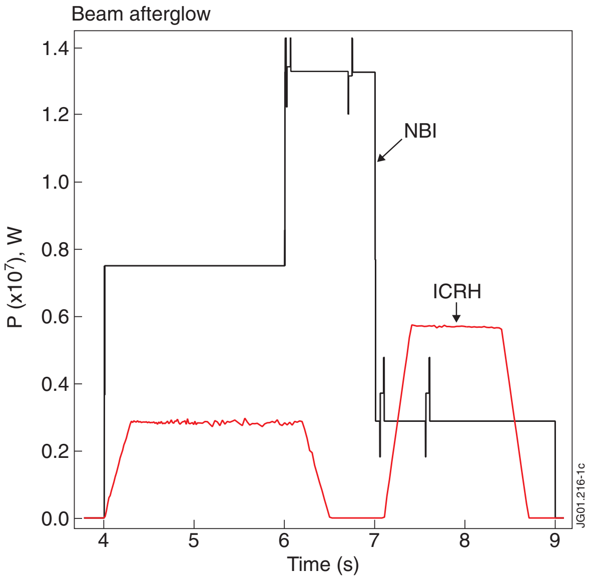

Figure 1: Temporal evolution of NBI and ICRH powers in optimised shear discharge (Pulse No: 52282) with B_T = 2.6 T and I_P = 2.2 MA.

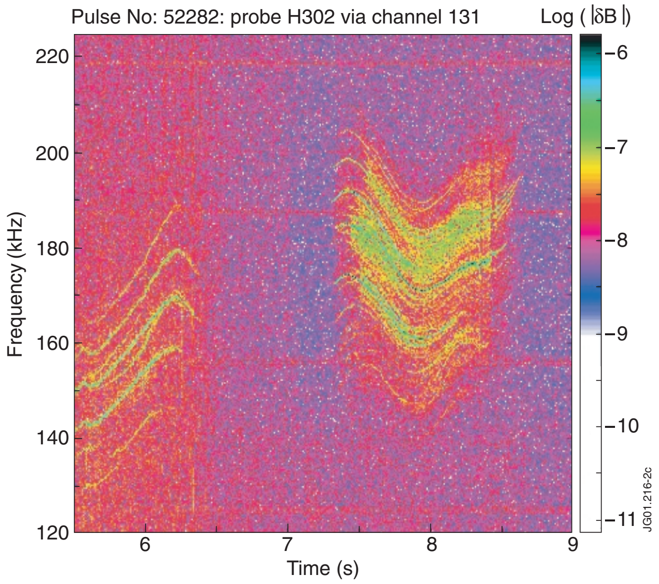

Figure 2: Spectrogram of magnetic perturbations, δB_P (Tesla), in Pulse *No: 52282 with monotonic q(r). TAEs are observed at 150-200 kHz during the afterglow phase, t=47.3-48.6s*

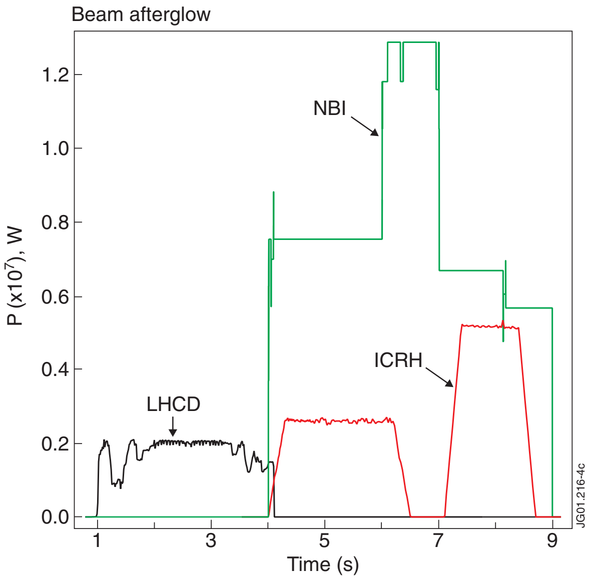

Figure 3: Temporal evolution of LHCD, NBI and ICRH in Pulse No: 52275 with B_T = 2.6T and I_P = 2.2MA.

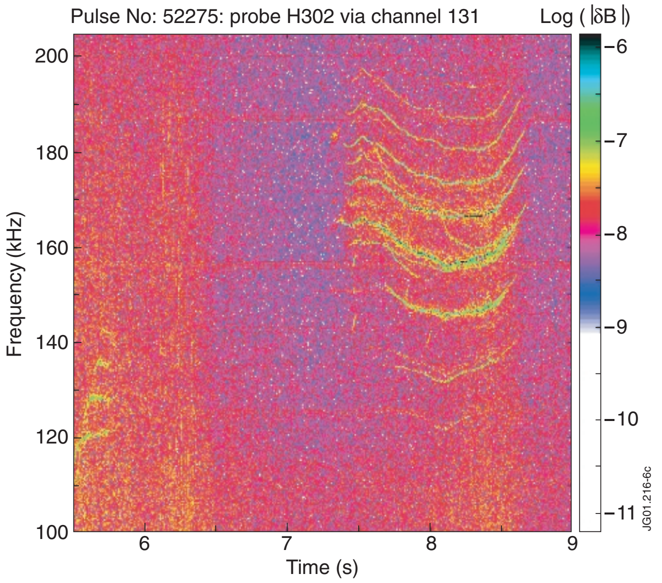

Figure 4: Spectrogram of the magnetic perturbations, in Pulse No: 52275 with nonmonotonic q(r).

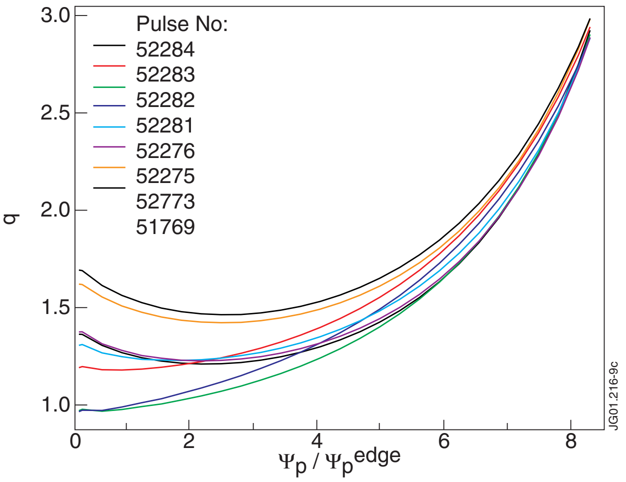

Figure 5: Safety factor profiles reconstructed from EFIT with MSE measurements for the beam afterglow experiments.

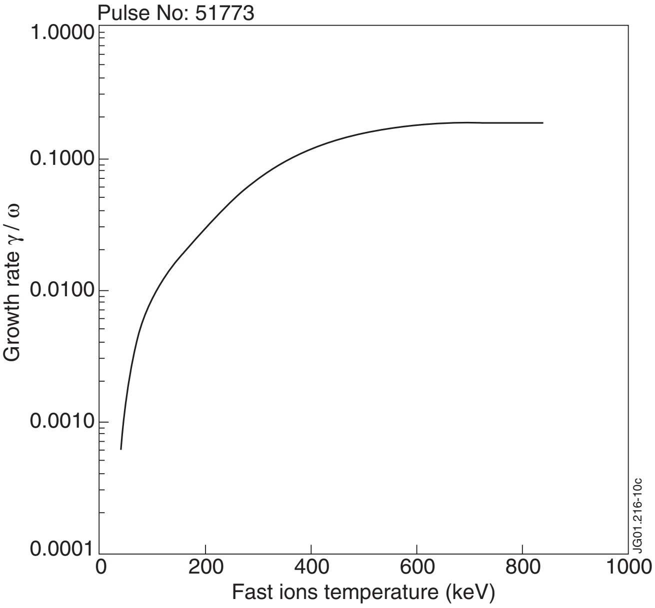

Figure 6: Normalised growth rate computed by the CASTOR-K code for the TAE.